# Polarity of Lipid Bilayers. A Fluorescence Investigation

Etienne Pérochon, André Lopez, and J. F. Tocanne*

*Centre de Recherche de Biochimie et Génétique Cellulaires du CNRS, 118 Route de Narbonne, F-31062 Toulouse Cedex, France*

*Received March 5, 1992; Revised Manuscript Received June 2, 1992*

ABSTRACT: Through steady-state and time-resolved fluorescence experiments, the polarity of the bilayers of egg phosphatidylcholine vesicles was studied by means of the solvatochromic 2-anthroyl fluorophore which we have recently introduced for investigating the environmental micropolarity of membranes and which was incorporated synthetically in phosphatidylcholine molecules (anthroyl-PC) in the form of 8-(2-anthroyl)octanoic acid. Fluorescence quenching experiments carried out with *N,N*-dimethylaniline and 12-doxylstearic acid as quenchers showed that the 2-anthroyl chromophore was located in depth in the hydrophobic region of the lipid bilayer corresponding to the $C_9$–$C_{16}$ segment of the acyl chains. Steady-state fluorescence spectroscopy revealed a nonstructured and red-shifted ($\lambda_{em}^{max}$ = 464 nm) spectrum for the probe in egg-PC bilayers, which greatly differed from the structured and blue ($\lambda_{em}^{max}$ = 404 nm) spectrum the fluorophore was shown to display in *n*-hexane. While the fluorescence decays of the fluorophore in organic solvents were monoexponential, three exponentials were required to account for the fluorescence decays of anthroyl-PC in egg-PC vesicles, with average characteristic times of 1.5 ns, 5.5 ns, and 20 ns. These lifetime values were independent of the emission wavelength used. Addition of cholesterol to the lipid did not alter these $\tau$ values. One just observed an increase in the fractional population of the 1.5-ns short-living species detrimental to the population of the 20-ns long-living ones. These observations enabled time-resolved fluorescence spectroscopy measurements to be achieved in the case of the 1/1 (mol/mol) egg-PC/cholesterol mixture. Three distinct decay associated spectra (DAS) were recorded, with maximum emission wavelengths, respectively, of 410 nm, 440 nm, and 477 nm for the 1.5-ns, 6-ns, and 20-ns lifetimes found in this system. On account of the properties and the polarity scale previously established for the 2-anthroyl chromophore in organic solvents, these data strongly suggest the occurrence of three distinct excited states for anthroyl-PC in egg-PC bilayers, corresponding to three environments for the 2-anthroyl chromophore, differing in polarity. The lifetime of 1.5 ns and the corresponding structured and blue ($\lambda_{em}^{max}$ = 410 nm) DAS account for a hydrophobic environment, with an apparent dielectric constant of 2, which is that expected for the hydrophobic core of the lipid bilayer. The lifetime of 5.5 ns indicates a more polar surrounding corresponding to an $\epsilon$ value around 2–20, the origin of which has still to be elucidated. In organic solvents, a lifetime of 20 ns was detected in the presence of water only. In egg-PC bilayers, this long lifetime, associated with a nonstructured and red-shifted ($\lambda_{em}^{max}$ = 477 nm) DAS, is suggested to account for interaction of the fluorophore with water molecules which diffuse across the bilayer. In connection with the dynamics of lipids in bilayers, these observations are discussed with regard to the permeability of lipid bilayers to water and its modulation by cholesterol and to the potential of the probe for investigating the polarity of membranes and their permeability to water.

Phospholipids take their ability to organize in the form of a bilayer in water from their amphiphilic structure. From an energetic viewpoint, this assembly is stabilized by a lattice of various dipolar and hydrogen bond forces of interaction between the polar head groups, including the water molecules of solvation, and by the hydrophobic effects which force the fatty acyl chains to aggregate (Tanford, 1973). The acyl chains form a hydrophobic core which is expected to have a low polarity. Thus, macroscopic approaches yield dielectric constant values around 2–4 for this region of the lipid bilayer, which are comparable to those found in alkanes (Tocanne & Teissié, 1990). The polar head group region, including the ester functions on the glycerol backbone, represents an interface between this hydrophobic region and the bulk of the water phase, with measured dielectric constant values in the range 10–45, greatly depending on the technique used (Tocanne & Teissié, 1990). This transition region corresponds to a very stiff gradient of polarity since the dielectric constant increases from its value of 2 in the hydrophobic core up to its value of 80 in water over a distance probably less than 1 nm (Flewelling & Hubbell, 1986; Tocanne & Teissié, 1990). X-ray and neutron diffraction data have enabled the hydrophobic/hydrophilic boundary in lipid bilayers to be located near the first $CH_2$ groups of the acyl chains (Knott & Schoenborn, 1986; Scherer, 1989; Simon & McIntosh, 1986; Wiener et al., 1991; Worcester & Franks, 1976). The hydrophobic core is responsible for the barrier properties lipid bilayers exhibit against the diffusion of water, solutes, and ions. However, it has long been recognized that, in artificial membranes, the lipid bilayer is not strictly impermeable to water (Bittman & Blau, 1972) and to small solutes like glycerol and sugar molecules (Demel et al., 1968, 1972). In particular, water exchanges rapidly between the exterior and the interior of lipid vesicles (Bittman & Blau, 1972; Finkelstein & Cass, 1968; Milon et al., 1986; Schuler et al., 1991; Träuble, 1971), implying the presence of water molecules within the hydrophobic core of the lipid bilayer. It has also been suggested that transient hydrogen-bonded chains of water molecules may account for the abnormally high conductivity of lipid bilayers to protons (Deamer & Bramhall, 1986; Deamer &

* To whom correspondence should be addressed.

0006-2960/92/0431-7672$03.00/0 © 1992 American Chemical Society

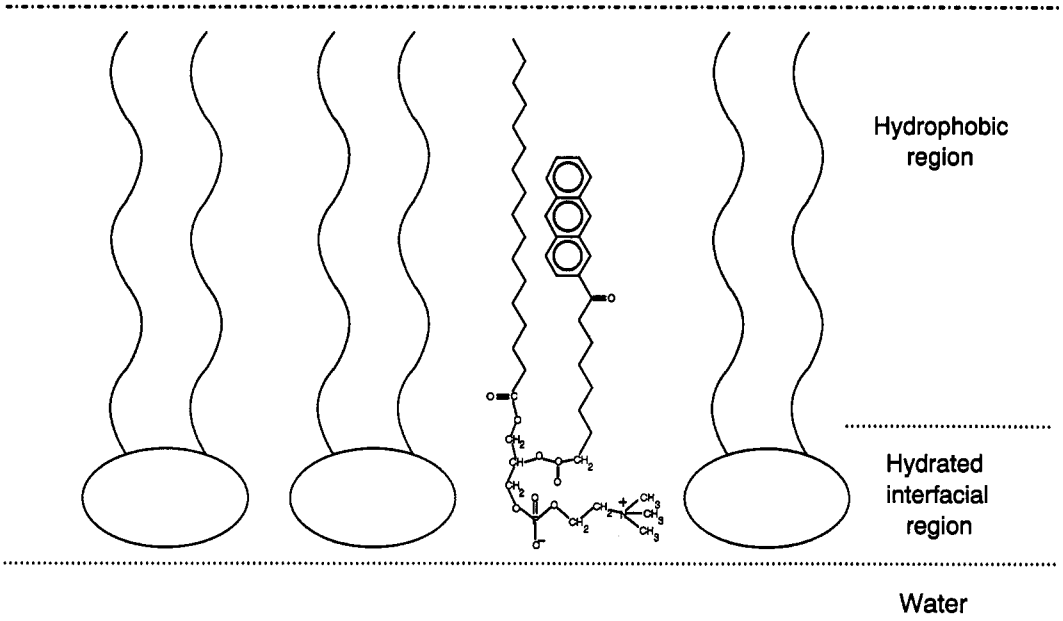


FIGURE 1: Chemical structure of anthroyl-PC and its insertion in a phospholipid bilayer.

Nichols, 1989; Nagle, 1987). It is clear that if the acyl chain region can be considered as being essentially hydrophobic in nature, an appreciation of its "polarity" will depend on the technique used. X-ray and neutron diffraction are macroscopic techniques which, in their very principle, cannot detect a few ill-localized water molecules, if present, in the hydrocarbon core of the bilayer. In contrast, the use of molecular probes is certainly one of the best suited approaches for scrutinizing membranes in terms of environmental micropolarity. An attempt to describe the shape of the hydrophobic barrier of phospholipid bilayers using electron spin labels has been reported (Griffith et al., 1974). In the same way, steady-state and time-resolved fluorescence spectroscopy can provide very interesting and complementary information on the polarity and dynamics of any medium, provided that well-suited and solvatochromic probes are available. In this respect, we have recently introduced the 2-anthroyl chromophore in the form of the 8-(2-anthroyl)octanoic acid (Pérochon & Tocanne, 1991) as a probe of polarity, because of the remarkable fluorescence properties it displays (Pérochon et al., 1991). Indeed, and owing to the presence of a keto group which is a hydrogen bond acceptor and which can conjugate with the aromatic ring so as to provide the chromophore with a high dipole moment, the fluorescence properties of the probe greatly depend on the polarity of the surrounding medium. Very large changes in Stokes shift, fluorescence lifetime, and quantum yield values are observed when going from hydrophobic to polar surroundings, and the effects of protic and aprotic solvents can easily be differentiated.

Phosphatidylcholine labeled with 8-(2-anthroyl)octanoic acid has been synthesized (anthroyl-PC,[1] Figure 1), and its phase properties and miscibility with other lipids have been carefully investigated (Pérochon & Tocanne, 1991). In the configuration used, where the aromatic rings and the polymethylenic chain lie along the same axis, anthracene was shown to be only slightly disturbing for the surrounding lipid phase and anthroyl-PC was shown to behave like a normal phospholipid, with good miscibility with lipids in the liquid phase (Pérochon & Tocanne, 1991). These results are similar to those previously reported for 9-(2-anthryl)nonanoic acid and corresponding anthrylphosphatidylcholines (de Bony & Tocanne, 1983).

In addition to the already reported potential of anthracene for investigating the lateral distribution (de Bony & Tocanne, 1984; de Bony et al., 1989) and motion (Dupou et al., 1988; Ferrières et al., 1989) of lipids in membranes, the phase behavior and the quite unique solvatochromic properties of 2-anthroyl-labeled phospholipids make these molecules a promising tool for studying the polarity of membranes. Before natural membranes were studied, it was important to get information first on the polarity of the lipid phase in membrane model systems. In the present study, and through steady-state and time-resolved fluorescence experiments, the probe anthroyl-PC embedded in egg phosphatidylcholine vesicles reveals the presence of water in the hydrophobic core of the lipid bilayer, which is modulated by cholesterol.

## MATERIALS AND METHODS

*Chemicals.* Synthesis of methyl 8-(2-anthroyl)octanoate and corresponding anthroyl-phosphatidylcholine (Figure 1) has been described (Pérochon & Tocanne, 1991). Egg yolk phosphatidylcholine was from Sigma Chemical Co. (St. Louis, MO). POPOP was purchased from Fluka (Buchs, Switzerland). *N,N*-Dimethylaniline was obtained from Prolabo (Paris, France) and was distilled in the presence of trifluoroacetic anhydride before to be used. Cholesterol was from Merck (Darmstadt, Germany). 12-AS, 16-AP, and 2-AP were from Molecular Probes Inc. (Eugene, OR). All solvents used were of spectrographic grade. They were obtained from Merck and used without further purification.

*Lipid Vesicles.* They were prepared using the method of reverse-phase evaporation described by Szoka et al. (1980).

*Fluorescence Spectrophotometry.* Uncorrected steady-state fluorescence spectra were recorded with a SLM-Aminco spectrofluorometer Model 500. In these experiments, the absorbance of the solutions was around 0.05 and never greater than 0.1. Absorption spectra were recorded with a Perkin-Elmer Lambda 5 UV/visible spectrometer.

[1] Abbreviations: anthroyl-PC, 1-acyl-2-[8-(2-anthroyl)octanoyl]-*sn*-glycero-3-phosphocholine; 2-AP, 2-AS, 3-AS, 6-AS, 9-AS, 12-AS, and 16-AP, *n*-(9-anthroyloxy) fatty acids where $n$ = 2, 3, 6, 9, 12, or 16; A, anthroyloxy; P, palmitic acid; S, stearic acid; DMA, *N,N*-dimethylaniline; DPH, 1,6-diphenyl-1,3,5-hexatriene; egg-PC: egg yolk phosphatidylcholine; POPOP, *p*-bis(5-phenyl-2-oxazolyl)benzene.

*Fluorescence Lifetime Determinations.* Nanosecond fluorescence decays were monitored using single photon counting techniques. Most of the experiments were carried out with the fluorometer Model 199 from Edinburgh Instrument (Edinburgh, Scotland, U.K.) equipped with monochromators on both the excitation and emission beams and using a coaxial flash lamp filled with nitrogen for excitation. An internal pressure of 1.5 atm and a distance between electrodes of 0.5 mm provided a flash of 1.5 ns width. Experiments were carried out with a flash repetition rate of 30 kHz. In order to avoid the color effect of the phototube, the apparatus response function was obtained after accumulation of the fluorescence decay of a short lifetime standard (POPOP in ethanol, $\tau$ = 1.35 ns) (Catteral & Duddel, 1983). The excitation wavelength was set at 337 nm using a monochromator with a slit width of 10 nm. A cutoff filter (KV 389; Schott, Germany) was interposed on the emission beam to reduce scattered excitation light. Decays were recorded over a time range of 200 ns dispatched over the 1024 channels of the multichannel analyzer. Analysis of the data was performed using a procedure which will be explained in detail elsewhere (A. Lopez, submitted for publication). Briefly, and after deconvoluting the flash lamp profile, fluorescence decays were analyzed as a sum of a finite number of exponentials using a least-square algorithm including a ponderation function accounting for the fact that the noise of photon counting obeys a Poisson law of distribution. Coupled with statistical analysis of the data, this procedure enabled us to calculate, for each exponential which composes a given fluorescence decay, its characteristic time $\tau_i$ and its steady state intensity $I_i$ according to the following equation:

$$I(t) = \sum_{i=1}^{i=n} I_i/\tau_i \exp(-t/\tau_i) \qquad (1)$$

with $\alpha_i = I_i/\tau_i$.

This approach enables the minimum and maximum values of these two parameters to be estimated, for a given error risk. In the following, all $\tau_i$ and $I_i$ values were calculated with an error risk of 5%.

Fluorescence decays were also obtained in the Laboratoire d'Utilisation des Rayonnements Electromagnétiques (LURE, Orsay, France), with an experimental setup coupled to the powerful pulsed light beam provided by the synchrotron radiation machine Super-ACO (SA1 window) (Kuipers et al., 1991). In our experiments, the storage ring provided a light pulse with a full width at half maximum of ~500 ps, at a frequency of 8.33 MHz for a double bunch mode. Bandwidths for excitation and emission were set at 5 nm and 10 nm, respectively. Photon counting was stopped when around $10^5$ counts were stored in the peak channel of the fluorescence intensity decay. The instrument response function was automatically monitored by measuring alternatively the fluorescence decay and the light scattered by the sample at the emission wavelength. Analysis of the fluorescence decays was performed using the maximum entropy method (Livesey & Brochon, 1987) or the approach described above.

*Fluorescence Quenching Experiments.* These experiments were carried out at 20 °C with probe molecules in solution in organic solvents (dichloromethane, ether, acetone, dimethylformamide/water, and ethanol/water mixtures) or embedded in egg-PC vesicles. In an organic solvent, probes (2-AP, 12-AS, 16-AP, methyl 8-(2-anthroyl)octanoate) were dissolved at a concentration of $10^{-5}$ M. With lipid vesicles, the concentration of the probes in the lipids was 0.5% (mol/mol), and lipids were dispersed in a 0.1 M phosphate buffer at pH 7.8. Lipid concentration was $5.9 \times 10^{-4}$ M.

Aliquots of the quenching solution (5 $\mu$L of a 1.6 M DMA solution in the organic solvent of reference or 10 $\mu$L of a 39 mM DMA aqueous solution at pH 2) were added stepwise to the various samples (2 mL of an organic solution or lipid suspension). At each step, and after homogenization ofthe solution, fluorescence spectra of the probes ($\lambda_{exc}$ = 340 nm, $\lambda_{em}$ = 380–650 nm) were recorded and photon counting experiments were carried out. The final DMA concentration was 23 mM in organic solvents and 0.58 mM for experiments with lipid vesicles.

*Time-Resolved Fluorescence Spectra.* Experiments were carried out with a fluorometer Model 199 from Edinburgh Instrument equipped with a timer (Model 719; EG&G Ortec, Princeton, NJ) coupled to a motor-driven monochromator on the emission beam for monitoring the emission wavelength. The various decay associated spectra (DAS), which are the fluorescence spectra associated to the various excited states of the probe in a given sample, were obtained using a procedure adapted from that published by Knutson et al. (1982). Experiments consisted in recording first as many time-resolved emission spectra (TRES) as there are the number $x$ of fluorescence lifetimes detected for the probe. Then, and using a set of $x$ linear equations combining the various measured $\tau_i$ and $I_i$ values, each DAS was obtained from the $x$ TRES by computing, at each wavelength step, the contribution of each excited state of the chromophore to the photon counting. A new algorithm was developed in our laboratory, enabling the computation of five DAS to be carried out.

For TRES recording, the emission wavelength was stepwise incremented by 0.43 nm. At each step, and via the time amplitude converter (TAC), the photons emitted between times $t_1$ and $t_2$, around one of the $x$ lifetimes identified in the sample under investigation ($t_1 < \tau_i < t_2$), were counted for 1 min and then stored successively in the various channels of the multichannel analyzer (MCA). Slit widths of 2 nm were used in the excitation and emission monochromators.

The three TRES shown in Figure 5 for 1 mol % anthroyl-PC in 1/1 (mol/mol) egg-PC/cholesterol mixtures, were recorded between 380 nm and 580 nm. Time windows (from the signal START of the TAC) of 25.8–35.3 ns, 35.7–48.8 ns, and 50–190 ns were used respectively for the three lifetimes of 1.5 ns, 6 ns, and 20 ns found for the probe in this lipid mixture. Around 500 counts were accumulated at each wavelength step in the most populated channel. This was enough for a correct evaluation of the DAS.

## RESULTS

*Fluorescence Excitation and Emission Spectra.* As mentioned in the introduction, the 2-anthroyl chromophore is endowed with remarkable properties of solvatochromism. Its fluorescence properties (Stokes shifts, lifetime $\tau$, and relative quantum yield $\phi_f$) have been carefully investigated in the case of methyl 8-(2-anthroyl)octanoate, in a large variety of solvents covering a large scale of polarity (Pérochon et al., 1991). Briefly, and as shown in Figure 2 and Table I, the fluorescence of the probe is greatly affected by the polarity of the surrounding medium. Thus, structured spectra were obtained in *n*-hexane (Figure 2a) and in other solvents of low polarity (benzene, diethyl ether, and ethyl acetate) (Pérochon et al., 1991). When more polar solvents like dimethylformamide were used, (Figure 2b), structureless and red-shifted emission spectra were recorded. The maximum emission wavelength $\lambda_{em}^{max}$ shifted from 404 nm in *n*-hexane to 448 nm in dimeth-

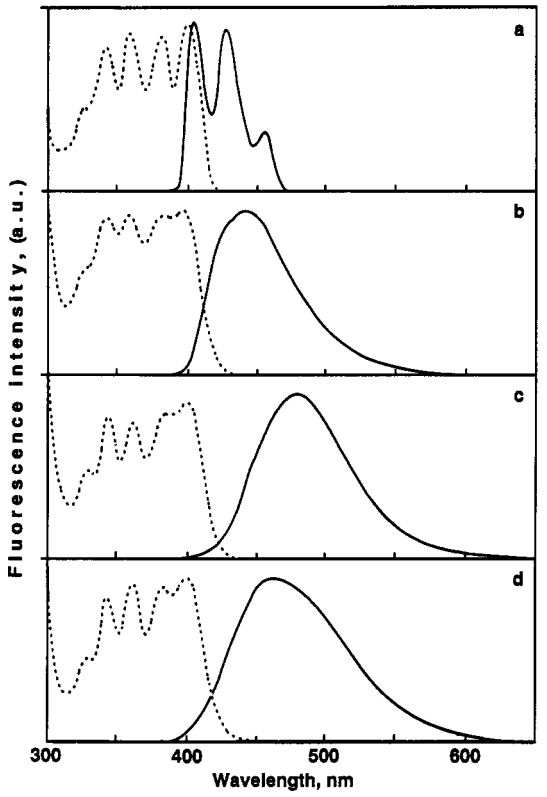


FIGURE 2: Normalized fluorescence excitation (- - -) and emission (—) spectra of methyl 8-(2-anthroyl)octanoate in *n*-hexane (a), dimethylformamide (b), dimethylformamide/water (3.9/6.1 mol/mol) mixtures (c) and of anthroyl-PC (1 mol %) in egg-PC vesicles (d). $\lambda_{em}$ values were 430 nm, 440 nm, 475 nm, and 460 nm, respectively, for the excitation spectra and $\lambda_{ex}$ was 340 nm for the emission spectra. The temperature was 20 °C.

ylformamide while the lifetime $\tau$ increased from 0.91 ns to 10.96 ns (Table I). In a concomitant way, the relative quantum yield $\phi_r$ increased from 1 to 18.8 (Pérochon et al., 1991). Addition of water to a solution of the probe in dimethylformamide resulted in a further bathochromic shift of its fluorescence emission spectra (Figure 2c). Extrapolating to 100% water, the data obtained for various dimethylformamide/water mixtures led to estimated values of 526 nm for $\lambda_{em}^{max}$, 27 for $\phi_r$, and 20 ns for $\tau$ in water (Pérochon et al., 1991).

It is worth stressing that these very large $\tau$, $\phi_r$, and Stokes shift values, in particular a lifetime of 20 ns, were characteristic of the probe in interaction with water. This would greatly facilitate the detection of water in any system.

With these properties in mind, anthroyl-PC was used for investigating the polarity of bilayers of egg-PC. First, it should be remembered that anthroyl-PC is miscible with lipids when in the liquid phase (Pérochon & Tocanne, 1991) and that egg-PC is a lipid which is in the liquid state at the temperature of 20 °C used for these experiments. As previously described, the excitation spectra of anthroyl-PC (Figure 2d) clearly accounts for a random distribution of the probe molecules within the host lipid (Pérochon & Tocanne, 1991). A structureless emission spectra was recorded (Figure 2d), with a maximum emission wavelength $\lambda_{em}^{max}$ around 464 nm. On account of the polarity scale established for the 2-anthroyl chromophore in organic solvents (Pérochon et al., 1991), such a high $\lambda_{em}^{max}$ value greatly suggests a polar environment for the probe in the lipid bilayer.

*Time-Resolved Fluorescence Spectroscopy.* To go further in this study, fluorescence lifetimes of anthroyl-PC embedded in egg-PC vesicles were determined. As shown in Table I, three exponentials with $\tau$ values around 1.1–2 ns, 5–7 ns, and 20–21 ns were required for a correct description of the fluorescence decays. This is in contrast to the behavior of the 2-anthroyl chromophore in organic solvents, where very good fits to decay data were obtained using a single exponential (Pérochon et al., 1991). In order to confirm the existence of three discrete excited states for the probe in lipid vesicles, suggested by these data, the same samples were submitted to photon counting experiments with the synchrotron machine in LURE and analyzed using the maximum entropy method (Livesey & Brochon, 1987). Note that in this approach the algorithm used first considers a large collection of 150 exponentials with different $\tau$ values of equal weight. At the end of the computation, it gives the distribution of the $\tau_i$ values which have to be retained for the best fitting to the decay data. Three narrow distributions were obtained, with central $\tau_i$ values of 2.05 ns, 4.71 ns, and 20.06 ns, very similar to those shown in Table I and determined using three discrete exponentials, as described above.

Interestingly and of great importance for the following, these $\tau_i$ values of 1.1–2 ns, 5.6 ns, and 20–21 ns remained unchanged when the fluorescence decays were recorded at wavelengths of 410 nm, 430 nm, 440 nm, and 450 nm, indicating that the three lifetimes found for the probe in egg-PC vesicles were independent of the fluorescence emission wavelength. As another control experiment, these lifetimes and the corresponding steady-state intensity $I_i$ values were found to remain unchanged when the probe concentration was increased up to 5 mol % in the lipid bilayers. This is to be related to our previous observation of complete miscibility of anthroyl-PC in egg-PC over the concentration range 0–5 mol % (Pérochon & Tocanne, 1991). In the following and unless otherwise specified, these three lifetimes will be referred to as their average values of 1.5 ns, 5.5 ns, and 20 ns, for the sake of clarity.

Because a lifetime of 20 ns might reflect the presence of water molecules in the lipid bilayer, it was interesting to test the influence of cholesterol on the system. As can be seen in Figure 3, addition of cholesterol to the lipids brought about a blue shift in the fluorescence emission maximum, with restoration of a structured spectrum. As shown in Table I and in Figure 4A, the three lifetimes found for anthroyl-PC in egg-PC alone remained unchanged. An increase in the fractional intensity of the 1.5-ns and to a lesser extent of the 5.5-ns short-living species was observed, detrimental to the 20-ns long-living ones. Note that these fractional intensities were determined at an emission wavelength of 440 nm, where each of the three decays was found to contribute significantly to the total fluorescence.

To go further in the interpretation of these results, time-resolved fluorescence spectra (TRES) were recorded in the case of the 1/1 egg-PC/cholesterol mixture. Such experiments could be envisaged because the three lifetimes of 1.5 ns, 6 ns, and 20 ns are quite different in value, independent of the emission wavelength, and of similar weight in this system. As can be seen in Figure 5, three well-differentiated decay associated spectra (DAS) were obtained for each lifetime: a blue and structured spectrum for the 1.5-ns short lifetime, with a $\lambda_{em}^{max}$ of 410 nm and two nonstructured green and yellow spectra with $\lambda_{em}^{max}$ values of 440 nm and 477 nm for the 6-ns and 20-ns lifetimes, respectively.

These observations point to the existence of three different excited states for the probe in the lipid bilayers, corresponding to three environments of distinct polarity.

Table I: Fluorescence Lifetimes, $\tau$ (ns), and Normalized Fractional Steady-State Fluorescence Intensities, $I_i$, for methyl 8-(2-Anthroyl)octanoate in *n*-Hexane [Taken from Pérochon et al. (1991)], Dimethylformamide, and Dimethylformamide/Water Mixtures and for Anthroyl-PC (1 mol %) in Vesicles of Egg-PC and Egg-PC/Cholesterol Mixtures[a]

| solvent | molar ratio | $\lambda_{em}^{max}$ | $\lambda_{fd}$ | $n$ | min $\tau_i$ (ns) | $\tau_i$ (ns) | max $\tau_i$ (ns) | $I_i$ | $\chi^2_r$ |
|---|---|---|---|---|---|---|---|---|---|
| *n*-hexane | | 404 | 430 | 1 | 0.8 | 0.91 | 1.0 | 1.0 | 1.60 |
| DMF | | 447 | 460 | 1 | 10.41 | 10.96 | 11.51 | 1.0 | 1.36 |
| DMF/$H_2O$ | 8.6/1.4 | 452 | 460 | 1 | 11.41 | 12.01 | 12.61 | 1.0 | 2.23 |
| | 6.7/3.3 | 458 | 460 | 1 | 15.04 | 15.83 | 16.63 | 1.0 | 1.33 |
| | 5/5 | 464 | 460 | 1 | 16.90 | 17.79 | 18.68 | 1.0 | 2.45 |
| | 3.9/6.1 | 475 | 460 | 1 | 18.22 | 19.19 | 20.15 | 1.0 | 1.09 |
| | 3.3/6.7 | 484 | 460 | 1 | 18.29 | 19.25 | 20.21 | 1.0 | 1.14 |
| | 2/8 | 495 | 460 | 1 | 18.64 | 19.63 | 20.61 | 1.0 | 1.25 |
| | 1.7/8.3 | 503 | 460 | 1 | 18.67 | 19.65 | 20.63 | 1.0 | 1.72 |
| egg-PC vesicles | | 464 | 450 | 3 | 20.01 | 21.06 | 22.12 | 0.80 | 1.30 |
| | | | | | 5.35 | 5.94 | 6.54 | 0.18 | |
| | | | | | 1.70 | 2.00 | 2.30 | 0.02 | |
| egg-PC/cholesterol vesicles | 9/1 | 463 | 450 | 3 | 20.54 | 21.63 | 22.71 | 0.79 | 1.10 |
| | | | | | 4.74 | 4.99 | 5.24 | 0.17 | |
| | | | | | 1.09 | 1.28 | 1.47 | 0.04 | |
| | 8/2 | 461 | 450 | 3 | 20.15 | 21.21 | 22.27 | 0.75 | 1.10 |
| | | | | | 5.21 | 5.49 | 5.76 | 0.19 | |
| | | | | | 1.14 | 1.34 | 1.55 | 0.06 | |
| | 7/3 | 458 | 450 | 3 | 19.78 | 20.82 | 21.87 | 0.70 | 1.12 |
| | | | | | 5.08 | 5.35 | 5.62 | 0.23 | |
| | | | | | 1.08 | 1.19 | 1.38 | 0.07 | |
| | 6/4 | 443 | 450 | 3 | 18.33 | 19.29 | 20.25 | 0.63 | 1.55 |
| | | | | | 4.94 | 5.26 | 5.52 | 0.29 | |
| | | | | | 1.02 | 1.13 | 1.25 | 0.08 | |
| | 5/5 | 438 | 450 | 3 | 18.99 | 20.00 | 20.99 | 0.59 | 1.22 |
| | | | | | 5.78 | 6.09 | 6.39 | 0.28 | |
| | | | | | 1.35 | 1.50 | 1.65 | 0.13 | |

[a] In all of these experiments, the excitation wavelength was 337 nm. $\lambda_{em}^{max}$ is the maximum emission wavelength. $\lambda_{fd}$ is the emission wavelength used for recording the fluorescence decays. $n$ is the number of exponentials used for fitting to the decay curves. $\tau$ values are given with an error risk of 5%.

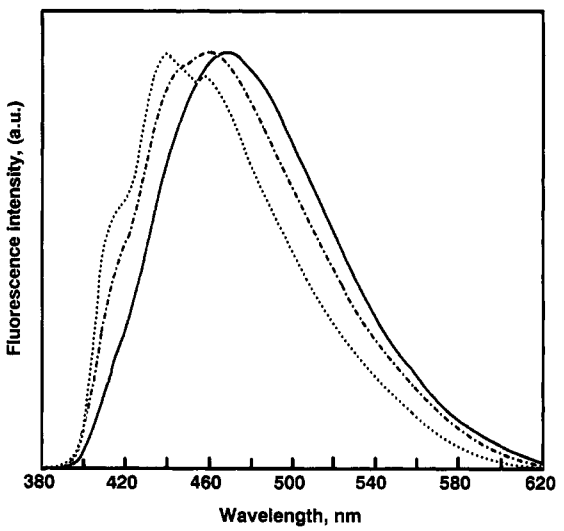


FIGURE 3: Normalized fluorescence emission spectra for anthroyl-PC (1 mol %) in vesicles of egg-PC/cholesterol mixtures, in the molar ratios 1/10 (—), 7/3 (– · –), and 1/1 (···). $\lambda_{ex}$ was 340 nm, and the temperature was 20 °C.

*Fluorescence Quenching Experiments.* A comparative study of the quenching properties of anthroyl-PC and *n*-(9-anthroyloxy) fatty acids (2-AP, 12-AS, and 16-AP) in egg-PC vesicles, by cupric ions as quenchers, showed that the 2-anthroyl chromophore was buried in the hydrophobic core of the lipid bilayer. Meanwhile, it appeared that the 2-anthroyl chromophore was less efficiently quenched by cupric ions than the 9-anthroyloxy group. It was then important to confirm this probe location using more efficient quenchers. Acrylamide, iodide, bromide derivatives, 12-doxylstearic acid, and *N*,*N*-dimethylaniline (DMA) were tested. Only the last two, and mainly DMA, gave significant quenching rates. For that reason, experiments were carried out with DMA as described below and using the following arguments.

First, in neutral and basic media, DMA is deprotonated, and only the deprotonated form of the molecule can penetrate lipid bilayers and is active as a fluorescence quencher (Sikaris et al., 1981). Because of its hydrophobic character and due to the orientational and motional anisotropy of the hydrocarbon phase in bilayers, deprotonated DMA partitions from the water phase into the lipid phase and accumulates in the region of high mobility of the acyl chains ($C_9$–$C_{16}$ carbon atom segment), with a concentration gradient increasing from the hydrophilic water/lipid interface toward the hydrophobic interior of the bilayer. This is supported by a theoretical analysis of solute partitioning into the acyl chains of lipid bilayers (Marqusee & Dill, 1986) and by quenching experiments carried out with a set of *n*-(9-anthroyloxy) fatty acids. These fluorescent probes, which are located at graded depths in egg-PC bilayers (Blat & Sawyer, 1985; Thulborn et al., 1979; Villalain & Prieto, 1991), are quenched by DMA with the increasing order of efficiency 2-AP < 12-AS < 16-AP (Sikaris et al., 1981). Control quenching experiments carried out in our laboratory with DMA and the same probes embedded in the same lipid led to similar results. On these grounds, one can assume that fluorescent probes located at the same depth in the lipid bilayer would experience the same DMA local concentration and therefore be quenched to the same extent, of course after being corrected for their respective quenching constants.

Usually, dynamic fluorescence quenching is accounted for using the Stern–Volmer equation:

$$I_0/I - 1 = k_q\tau_0[Q] \quad (2)$$

where $I$ and $I_0$ are the fluorescence intensities measured in the presence and in the absence of quencher respectively, $k_q$ is the bimolecular quenching constant, $\tau_0$ is the fluorescence lifetime of the chromophore in the absence of quencher, and [Q] is the quencher concentration (Lakowicz, 1983).

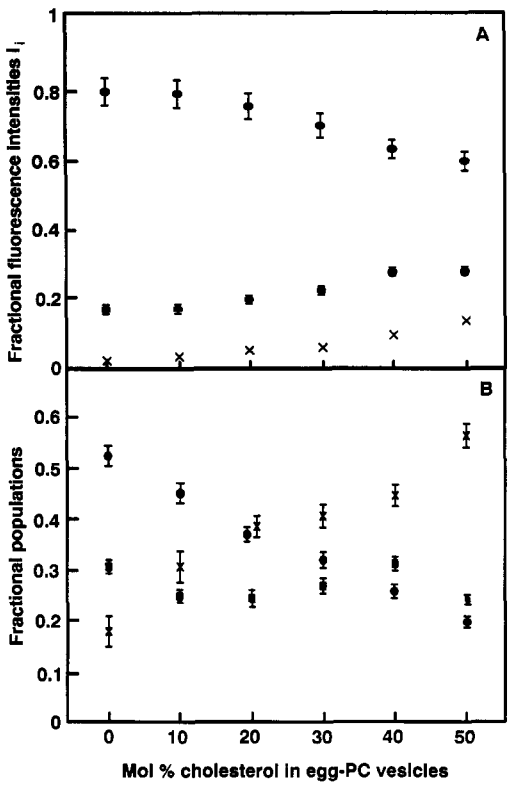


FIGURE 4: Effect of cholesterol (A) on the fractional fluorescence intensities $I_i$ and (B) on the fractional probe populations corresponding to the three lifetimes of 1.5 ns (×), 5.5 ns (■), and 20 ns (●) found for anthroyl-PC (1 mol %) in egg-PC vesicles. Data in (A) were recorded at an emission wavelength of 440 nm where each of the three decays was found to contribute significantly to the total fluorescence. Data in (B) were obtained after correcting the three sets of $I_i$ values in (A) by the relative quantum yields values of 2, 10, and 26 which can be respectively associated to the lifetimes of 1.5 ns, 5.5 ns, and 20 ns (Pérochon et al., 1991). Fractional intensities and populations were estimated with an error risk of 5%.

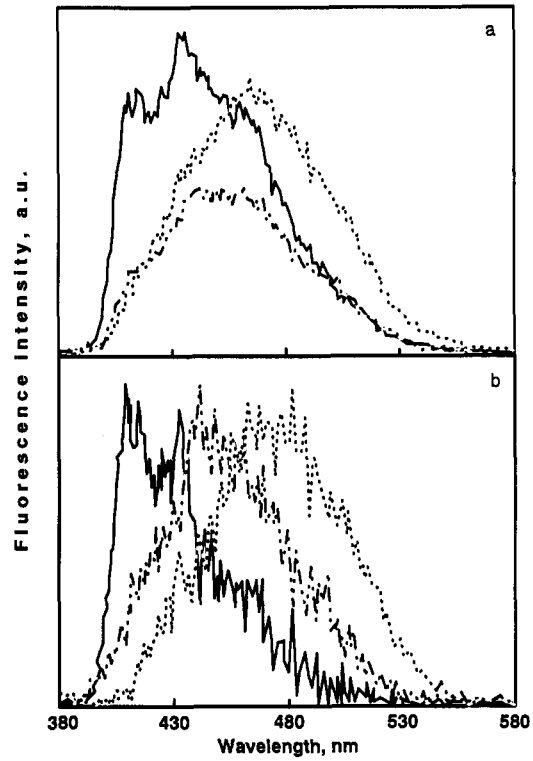


FIGURE 5: Time-resolved emission spectra (a) and decay associated spectra (b) obtained for the three lifetimes of 1.5 ns (—), 6 ns (– ··), and 20 ns (···) found for anthroyl-PC (1 mol %) in vesicular suspensions of 1/1 (mol/mol) egg-PC/cholesterol mixtures.

This approach is valid only for a fluorescence emission associated with a single fluorescence lifetime. It does not apply to anthroyl-PC in egg-PC, where three lifetimes were observed. In this case, it is preferable to consider the changes in lifetimes which result from the quenching process, by using

$$\tau_{i,0}/\tau_i - 1 = k_q \tau_{i,0}[Q] \qquad (3)$$

where $\tau_{i,0}$ and $\tau_i$ represent the fluorescence lifetime of the $i$th emitting species in the absence and in the presence of quencher, respectively.

Difficulties can arise if diffusional effects limit the collision rate between the encounters since, in this case, the fluorescence decays can no longer be exponential in nature (Lakowicz et al., 1987). In fact, in all the quenching experiments which we have carried out with DMA, in organic solvents and in lipid vesicles, decays remained very well described using one or a sum of discrete exponentials.

To account for the possibility that the three lifetimes of anthroyl-PC in lipid vesicles were not necessarily quenched to the same extent by DMA, control quenching experiments were first carried out with methyl 8-(2-anthroyl)octanoate dissolved in ether and acetone and in dimethylformamide/water 3.9/6.1 (mol/mol) and ethanol/water 7.2/2.8 (mol/mol) mixtures. These solvents were chosen for their polarity, in order to obtain lifetimes of 1.5 ns, 5.5 ns, and 20 ns for the probe and fluorescence emission spectra similar to the three corresponding DAS in Figure 5. In each solvent system, fluorescence decays were monoexponential and the corresponding lifetimes $\tau$ were observed to decrease with increasing DMA concentration, indicating a predominant collisional quenching process. From eq 2, these quenching data yielded quenching constants $k_q$ of $2.5 \times 10^{10}$ $M^{-1}$ $s^{-1}$ in ether, of $2.3 \times 10^{10}$ $M^{-1}$ $s^{-1}$ in acetone, and of $0.48 \times 10^{10}$ $M^{-1}$ $s^{-1}$ in dimethylformamide/water and ethanol/water mixtures. This showed that the 2-anthroyl chromophore was less easily quenched by DMA when associated with water than when dissolved in aprotic media.

Addition of DMA to vesicles of 0.5 mol % anthroyl-PC in egg-PC brought about a decrease in the fluorescence intensity of the probe, with a blue shift of its emission spectra (not shown) and a decrease in the three fluorescence lifetimes (Figure 6).

Because the microviscosity in the bulk of an organic solvent more than likely differs from that of the hydrocarbon chains in the bilayer, the diffusion rate of DMA and therefore the bimolecular rate constant for dynamic quenching are unlikely to be the same in the two systems. Consequently, the quenching constants $k_q$ measured for the 2-anthroyl chromophore in organic solvents are not directly transposable to lipid bilayers. However, they can reasonably be assumed to be similar in relative values, thus enabling eq 3 to be used to evaluate, for each DMA concentration in the external water phase, the local DMA concentration which, in the bilayer, affects each lifetime. In the following, these local DMA concentrations in the bilayer will be referred to as "bulk equivalent" DMA concentrations [BEQ-DMA]'s. Results of these calculations, carried out using the quenching data of Figure 6 and the above $k_q$ values determined for each lifetime in organic solvents, are shown in Figure 7. Within the experimental errors which are inherent to this type of experiment and which affect more particularly the short lifetimes and the low quencher concentrations, the three lifetimes found for anthroyl-PC in egg-PC bilayers were affected by similar [BEQ-DMA]'s. Thus,

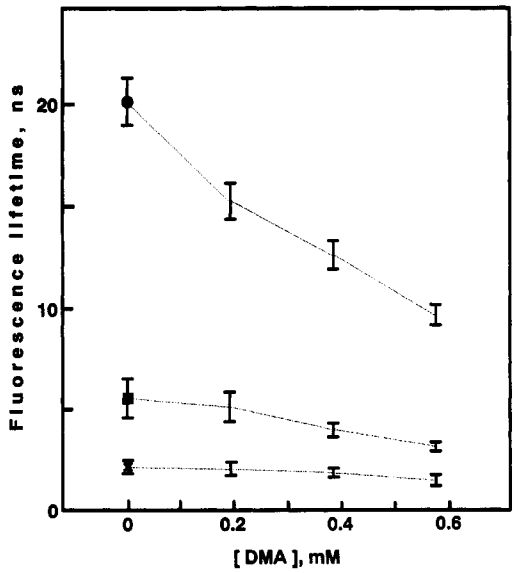


FIGURE 6: Changes in the three fluorescence lifetimes of anthroyl-PC (1 mol %) in egg-PC vesicles, upon addition of *N,N*-dimethylaniline to the water phase. Lifetimes were 2.2 ns (×), 5.53 ns (■), and 20.16 ns (●) in the absence of DMA. The pH of the solution was 7.8, and the temperature was 20 °C. $\lambda_{ex}$ was 337 nm, and $\lambda_{em}$ was 440 nm.

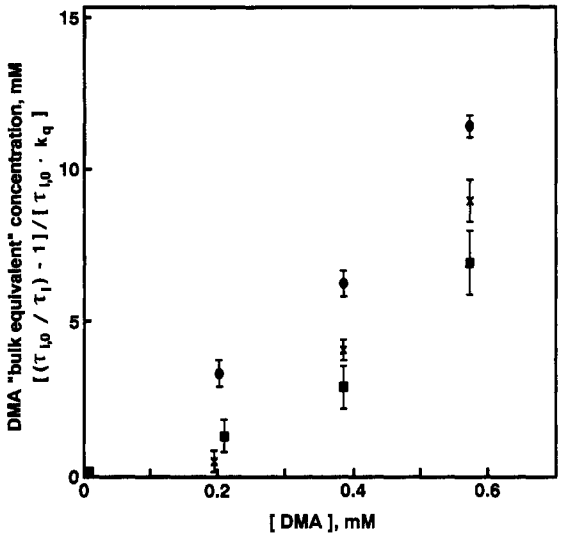


FIGURE 7: Relationship between the external concentration of *N,N*-dimethylaniline in the aqueous phase and its local or "bulk equivalent" concentration in the hydrophobic region of egg-PC bilayers containing 1 mol % of anthroyl-PC. Calculations were carried out for the three lifetimes of 1.5 ns (×), 5.5 ns (■), and 20 ns (●) which characterize the system and by using eq. 3, with the lifetime values given in Figure 6, and a quenching constant of $2.5 \times 10^{10}$ $M^{-1}$ $s^{-1}$, $2.3 \times 10^{10}$ $M^{-1}$ $s^{-1}$, and $0.48 \times 10^{10}$ $M^{-1}$ $s^{-1}$ for the 1.5-ns, 5.5-ns, and 20-ns lifetimes respectively.

for an external DMA concentration of 0.57 mM, [BEQ-DMA] values of 9 mM, 7 mM, and 11.6 mM were estimated for the lifetimes of 1.5 ns, 5.5 ns, and 20 ns, respectively, indicating a 14–20-fold increase in the DMA concentration in the bilayer as compared to in the aqueous phase. Although underestimated, this value of 20 for the partition coefficient of DMA in egg-PC vesicles (estimated with respect to the 20-ns lifetime) seems to be quite reasonable. Indeed, the partition coefficients for a wide variety of anesthetic drugs and other solutes into bilayers and membranes have been reported to be 2–15-fold smaller than for the same solutes into oils (Marqusee & Dill, 1986); we measured a partition coefficient of 80 for DMA in *n*-hexane, by equilibration of the organic phase with a water phase at pH 7.8.

Finally and as another control experiment, the presence of 10 mol % of 12-doxylstearic acid in egg-PC vesicles containing 0.5 mol % anthroyl-PC brought about a 10% decrease in the fluorescence emission of anthroyl-PC with a concomitant decrease in the three lifetime values.

This and the above quenching experiments greatly support the conclusion that the various excited states of anthroyl-PC in egg-PC bilayers correspond to 2-anthroyl groups buried in the hydrophobic region of the lipid bilayer and located at the same depth.

## DISCUSSION

In agreement with our previous data (Pérochon & Tocanne, 1991), the present study shows that anthroyl-PC, when incorporated at low concentrations (0.5–1 mol %) in egg-PC vesicles, exhibits nonstructured fluorescence spectra with a maximum emission wavelength around 464 nm. If one just looks at this Stokes shift, and according to the polarity scale previously established for the 2-anthroyl chromophore in organic solvents, a $\lambda_{em}^{max}$ of 464 nm would account for a local dielectric constant around 35 (Pérochon et al., 1991). Such a conclusion is not that expected on consideration of the hydrophobic environment that the acyl chains of the host lipid would normally provide the probe with, and it looks rather unrealistic.

In fact, the lipid bilayer in the membrane cannot be considered as a medium with bulk physical properties. It does not provide an isotropic phase as encountered in the bulk of organic solvents, but rather an anisotropic phase in which the acyl chains are aligned perpendicular to the membrane surface. There is a gradient in molecular motion provided by the increasing probability of trans–gauche isomerization about carbon–carbon bonds as the center of the bilayer is approached, and recent molecular dynamics simulations strongly suggest that the chain disorder is much bigger than most textbook pictures of membranes might suggest (Egberts & Berendsen, 1988; De Loof et al., 1991). This can generate structural heterogeneities in the lipid structure corresponding to environmental micropolarities, and only time-resolved fluorescence spectroscopy can enable some valid predictions to be made on the polarity of the probe surroundings. It is also worth emphasizing that the dielectric constant is a macroscopic concept which has no unique meaning on the molecular scale (Flewelling & Hubbell, 1986; Raudino & Mauzerall, 1986).

Whichever the method of analysis used, the fluorescence decays of the probe in egg-PC vesicles, in both the absence and presence of cholesterol, were well accounted for using three discrete exponentials, with corresponding lifetimes of 1.5 ns, 5.5 ns, and 20 ns. These $\tau$ values appeared to be practically independent of the emission wavelength, thus indicating the presence of three distinct excited states for the 2-anthroyl chromophore and enabling the corresponding time-resolved fluorescence emission spectra (TRES) and decay associated spectra (DAS) to be recorded. These results are now to be discussed in connection with the location of the 2-anthroyl group in the bilayer, its fluorescence properties, and the dynamics of the bilayer assembly.

With respect to the chromophore location, one might argue that despite the high hydrophobicity of the anthracene moiety, the presence of a keto group might force the 2-anthroyl fluorophore to loop back from the center of the bilayer into the hydrated interfacial region of the lipid bilayer. In fact, and owing to the size and rigidity of the anthracene residue, partial looping back of the probe would require a rather large space between lipid molecules corresponding to a destabilization of

the lipid bilayer. This is in contradiction with the regular phase behavior anthroyl-PC was shown to exhibit, alone or when mixed with other lipids (Pérochon & Tocanne, 1991). It is now well established that the 9-anthroyloxy moiety in *n*-(9-anthroyloxy) fatty acids (2-AP, 2-AS, 3-AS, 6-AS, 9-AS, 12-AS, and 16-AP) is located at graded depths in lipid bilayers, from the interfacial region for $n = 2$ up to the center of the bilayer for $n = 16$ (Blatt & Sawyer, 1985; Thulborn et al., 1979; Villalain & Prieto, 1991). In terms of polarity, the ester bond and the keto group which differentiate the 9-anthroyloxy and 2-anthroyl chromophores are nearly equivalent. For example, ethyl acetate and acetone display similar partition coefficients from water to the hydrocarbon phase of dimyristoylphosphatidylcholine bilayers in the liquid state (Katz & Diamond, 1974). Therefore, the conclusion that the anthroyloxy group in 9-AS, 12-AS, and 16-AP is deeply buried in the hydrocarbon phase of bilayers should also apply to the 2-anthroyl chromophore in anthroyl-PC. As more direct evidence, no fluorescence quenching was observed when the nonpermeant cupric $Cu^{2+}$ ions were used as quenchers (Pérochon & Tocanne, 1991). Consistently, the quenching data obtained in the present study with 12-doxylstearic acid and principally with DMA also account for the presence of the fluorophore in the hydrophobic core of the bilayer. In addition, they greatly suggest that the three distinct fluorescence emissions detected for anthroyl-PC in egg-PC originate from 2-anthroyl groups located at the same depth in the bilayer.

In terms of fluorescence properties and as previously reported, the carbonyl group of the 2-anthroyl chromophore is coplanar with the aromatic ring in both the ground and excited states. This is the conformation of minimum energy which favors the conjugation between the carbonyl group and the aromatic ring and consequently provides the probe with a very high dipole moment in the excited state (Pérochon et al., 1991). This makes the probe rather insensitive to changes in molecular packing but, in contrast, very sensitive to the polarity of its environment and capable of discriminating between general solvent effects (dipolar solute/solvent interactions) and specific solvent effects (hydrogen bonding) in aprotic and protic environments, respectively (Pérochon et al., 1991). Thus, the short lifetime of 1.5 ns and the corresponding structured and blue DAS clearly account for a hydrophobic environment for the probe with a dielectric constant around 2, which is that expected for the hydrophobic region of the bilayer. A lifetime of 5.5 ns is intermediate between the values of 4.35 ns and 6.23 ns found for the probe in benzene ($\epsilon = 2.28$) and acetone ($\epsilon = 20.7$), respectively. The corresponding nonstructured DAS, with a $\lambda_{em}^{max}$ of 440 nm, would still account for an aprotic medium, but of higher polarity, with an $\epsilon$ value around 30. We have no straightforward interpretation to propose as to the origin of this intermediate lifetime. If one just considers its value of 5.5 ns, which suggests benzene-like or acetone-like environments for the probe, it might partly correspond to collisional encounterings of probe molecules in the bilayer. A lifetime of 20 ns is characteristic of a protic environment and was detected in the presence of water only (Pérochon et al., 1991). This large $\tau$ value and the corresponding nonstructured and red-shifted DAS, with a $\lambda_{em}^{max}$ of 477 nm, which, in fact, imposes its spectrum on the total spectrum of the probe in the bilayer, were mimicked when methyl 8-(2-anthroyl)octanoate was dissolved in DMF/water 3.9/6.1 (mol/mol) or ethanol/water 7.2/2.8 (mol/mol) mixtures. This clearly indicates that anthroyl-PC in egg-PC vesicles was interacting with water. Because of thermal fluctuations, the possibility for the 2-anthroyl group to reach sometimes the hydrated interfacial region of the bilayer, by translation along the bilayer normal, cannot be totally excluded a priori. In fact, the distribution of the double bonds at the 9–10 positions of the two acyl chains in dioleoylphosphatidylcholine and of water molecules in the interfacial region has been recently elucidated through a refined study of the X-ray and neutron diffraction data obtained for hydrated bilayers of the lipid (Wiener et al., 1991). These distributions are well accounted for by nonoverlapping Gaussian functions centered at a distance of 0.788 nm for the two double bonds, and of 0.225 nm for water, from the center of the bilayer. The keto group in anthroyl-PC also occupies the 9-position in the *sn*-2 acyl chain of the lipid and probably undergoes similar average thermal motions with respect to the bilayer normal. Consequently, the possibility for the 20-ns long-living species, which account for up to 80% of the total fluorescence intensity, to originate mainly from a large proportion of 2-anthroyl chromophores located in the hydrated interfacial region of the lipid bilayer can be discarded. In other words, this means that anthroyl-PC detects the presence of water in the hydrophobic region of egg-PC bilayers. The 2-anthroyl chromophore is known to exhibit a charge transfer character in the excited state, and the resulting increase in basicity of the carbonyl group is expected to favor specific hydrogen bond interactions with water and other protic molecules (Pérochon et al., 1991). These interactions with the keto group of anthroyl-PC indicate the presence of water around the 9-position of the hydrocarbon chains in egg-PC bilayers. This is the first time that water is detected so deeply in the hydrophobic region of a phospholipid bilayer.

Convincing experimental evidence indicating the presence of water within the hydrocarbon phase of lipid bilayers is still very scarce. As mentioned in the introduction, X-ray and neutron diffraction data have enabled the hydrophobic/hydrophilic boundary in lipid bilayers to be located near the first $CH_2$ groups of the acyl chains (Knott & Schoenborn, 1986; Scherer, 1989; Simon & McIntosh, 1986; Wiener et al., 1991; Worcester & Franks, 1976), but these diffraction techniques cannot detect the presence of ill-localized water molecules diffusing in the hydrocarbon core of the bilayer. Indirect evidence for the presence of water in the hydrophobic region of lipid bilayers has been inferred from fluorescence studies with DPH as a probe of environmental microheterogeneity in a large variety of lipid bilayers and membranes (Fiorini et al., 1987, 1988, 1989; Straum & Litman, 1987a,b; Williams & Stubbs, 1988; Zannoni, 1983; Zolese et al., 1990) and from the comparison of measured and estimated apparent molar heat capacities for aqueous dispersions of phospholipids (Blume, 1983).

As more direct evidence, the comparison of the ESR spectra of 5-, 12-, and 16-doxylstearic acids embedded in microsomal lipids from calf liver indicated the presence of water in position 5, but not in positions 12 and 16 of the acyl chains (Griffith et al., 1974). Quite recently, the analysis of the photoproducts of a lyso-$G_{M1}$ ganglioside derivative bearing a diazirinyl photoreactive group revealed the presence of water around the 7–9 carbon atoms of the acyl chains in egg-PC liposomes and calf brain microsomes (Meier et al., 1990).

The exact stoichiometry and lifetime of the anthroyl-PC/water interactions we have put forward are still to be elucidated. However, and because these interactions are more than likely to be thought in terms of hydrogen bonding, a large amount of water is not required. A probe to water molar ratio of 1/1 might be enough, corresponding in fact to the detection of single and isolated water molecules. Furthermore, and because

the probe lifetimes are independent of the emission wavelength, the lifetimes of these probe/water interactions must be comparable to that of the corresponding excited state for the probe, i.e., at least of 20 ns.

The possibility that the presence of water so detected might be a direct consequence of the incorporation of the probe in the lipid bilayer can be discarded since the three fluorescence lifetimes and their respective fractional populations were found to be independent of the probe concentration in the bilayer. Very likely, the presence of water within the lipid acyl chains is to be related to the high permeability to water phospholipid bilayers are known to display (Bittman & Blau, 1972). There are at least two models to explain the underlying mechanisms of water permeation (Deamer & Bramhall, 1986). The first was proposed to account for the abnormally high conductivity of lipid bilayers to protons (Deamer & Bramhall, 1986; Deamer & Nichols, 1989; Nagle, 1987). It considers the existence of transient hydrogen-bonded chains (tHBC) of water molecules along the bilayer normal, which would occassionally arise from thermal fluctuations in the lipid bilayer. The second, and probably most generally accepted, is the solubility–diffusion model. Water permeability is considered to arise from a process in which individual water molecules dissolve in the nonpolar region of the bilayer and cross by simple diffusion. As proposed by Träuble (1971), dissolution and diffusion of water molecules would be facilitated by the existence of kinks which form and diffuse due to $\beta$-coupled gauche–trans–gauche isomerization along the acyl chains of the lipids. It is not yet possible to choose between the two models, and our fluorescence data are compatible with both. The two models afford the probe with the possibility of interacting specifically with water molecules. Note that dipolar solute/solvent reorientations should be accounted for when considering the tHBC model. Nevertheless, the observation that water molecules in bulk alkane solvents would exist in the monomeric form and not hydrogen bonded to others in aggregates (Conrad & Strauss, 1985) brings strong support to the solubility–diffusion model. Using two different approaches, Träuble (1971) and Diamond and Katz (1974) arrived at the same formulation for the permeation coefficient $P$ of water through membranes, which can take the simplified form $P = K_p D/\delta$, where $K_p$ is the partition coefficient of water from the bulk of the aqueous phase to the lipid hydrocarbon phase, $D$ is the diffusion coefficient of water molecules in the lipid bilayer, and $\delta$ is the thickness of the bilayer to be crossed. Also in support of the solubility-diffusion model, this expression led to a calculated permeability coefficient very similar to those found experimentally when the partition and diffusion coefficients of water in alkanes were used (Finkelstein & Cass, 1968; Lipschitz-Faber & Degani, 1980; Träuble, 1971).

Finally and with respect to the lifetime of the probe/water interactions, recent molecular dynamics simulations indicate that if multiple trans–gauche isomerizations can occur in the acyl chains in the 100-ps time scale, a complete description of the various motions of one phosphatidylcholine molecule is achieved at the nanosecond time scale (De Loof et al., 1991). In addition, the anthracene moiety of the probe, because of its rigidity and planeity, is expected to increase the local acyl chain order and therefore to decrease the trans–gauche isomerization rate, while hydrogen bonding with the keto group would stabilize water molecules in the vicinity of the probe. Furthermore, water in the middle of lipid bilayers diffuses three times slower than bulk water (Egberts & Berendsen, 1988). These arguments make quite reasonable a lifetime of at least 20 ns for the probe/water interactions in the bilayer.

Cholesterol has long been recognized to decrease water permeation through phospholipid bilayers (Bittmann & Blau, 1972; Finkelstein & Cass, 1968; Milon et al., 1986; Schuler et al., 1991; Träuble, 1971). In this respect, it is quite interesting to observe that increasing the concentration of cholesterol in egg-PC bilayers brought about a decrease in the fractional intensity of the 20-ns long-living anthroyl-PC molecules associated with water. More precisely, and taking into account the relationships which have been established between lifetimes and quantum yields for the probe (Pérochon et al., 1991), relative fluorescence quantum yields of 2, 10, and 26 can be estimated for the three lifetimes of 1.5 ns, 5.5 ns, and 20 ns, respectively. Dividing the corresponding sets of fractional intensities in Figure 4A by their respective quantum yields enabled the fractional population of the various excited states of the probe, shown in Figure 4B, to be estimated. Note that data in panels A and B were obtained at the emission wavelength of 440 nm where the three decays were found to contribute significantly to the total fluorescence. It is remarkable to observe that the fractional population of probe molecules with a lifetime of 5.5 ns remained practically constant at around 25–30%, while the fractional population of probes with a lifetime of 20 ns decreased from 52% down to 20% and the fractional population of probes with the short lifetime of 1.5 ns increased from 17% up to 56%. In other words, this means that addition of cholesterol to the lipids reduced the number of anthroyl-PC molecules in contact with water. This can be interpreted along with the ordering effect cholesterol and other sterols have on membranes and which can be accounted for by an increase in the order parameter of the hydrocarbon chains of the lipid molecules (Schuler et al., 1991; Yeagle, 1985). Increasing the motional order of the acyl chains corresponds to a decrease in trans–gauche isomerization. Considering the solubility–diffusion model, this would bring about a decrease in the kink concentration and therefore in the partition coefficient of water in the hydrocarbon region of the bilayers (Träuble, 1971). In this respect and as shown in Figure 8, there is a remarkable parallelism between the cholesterol-mediated decreases in the population of those probe molecules which are associated with water and in the permeability to water of egg-PC vesicles, as measured for example by Bittman and Blau (1972) using osmotic gradients. In the absence of precise knowledge of the fluorescence emission mechanism of the probe in the presence of water, this strict parallelism in the decrease rate of the two parameters may be fortuitous. Nevertheless, this would suggest that the probe can be used as a direct reporter of the permeability of lipid bilayers to water.

Unfortunately, it is extremely difficult to evaluate the water concentration within the hydrophobic region of the bilayer from our fluorescence data. However, note that a concentration around 2–30 mM was evaluated by Meier et al. (1990), which lies in the range of the solubility of water in saturated or unsaturated alkanes.

Altogether, and in view of the solubility–diffusion model, the rather complex fluorescence data obtained for anthroyl-PC in egg-PC vesicles, in the absence and presence of cholesterol, can be interpreted in a self-consistent way. This allows us to conclude that 2-anthroyl chromophore experiences at least three different and quite distinct environments, two of hydrophobic nature and the third corresponding to interactions with water molecules diffusing across the lipid bilayer.

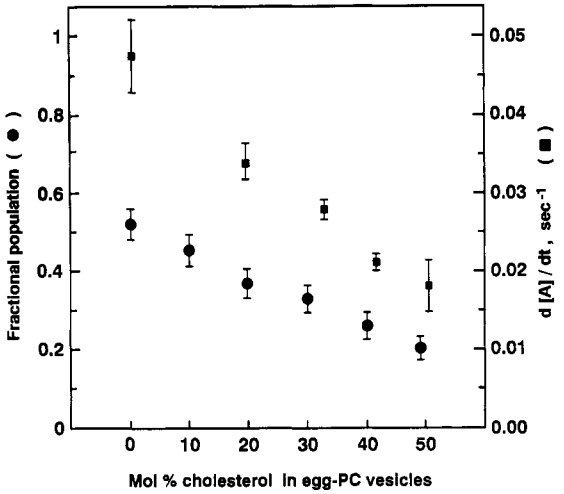


FIGURE 8: A comparison of the effect of cholesterol on the fractional population of the 20-ns long-living species of anthroyl-PC (1 mol %) in egg-PC vesicles (●) and on the initial rate $dA/dt$ (■) of the swelling of egg-PC vesicles submitted to an osmotic pressure gradient [data from Bittman and Blau (1972)]. The change in absorbance, $dA/dt$, which results from the osmotic swelling of liposomes represents a convenient means to measure the initial rate of their volume change, $dV/dt$, which itself has been shown to reflect the permeability coefficient of water to the lipid bilayer (Milon et al., 1986). The fractional populations of the long-living species of anthroyl-PC were taken from data in Figure 4B. They are given with an error risk of 5%.

It is worth emphasizing that like 9-(2-anthryl)nonanoic acid (Welby & Tocanne, 1982; Dupou et al., 1986), 8-(2-anthroyl)-octanoic acid can incorporate metabolically into the various membrane lipids of both prokaryotic (bacterium *Micrococcus luteus*) and eukaryotic (Chinese hamster ovary cells) cells in culture (unpublished data). This provides us with the great advantage of being able to study, in situ, the behavior of constitutive membrane lipids. In addition to the potential of the probe for reporting on membrane fluidity (Pérochon & Tocanne, 1991), the 2-anthroyl chromophore appears to be a promising tool for probing the organization of biological membranes in terms of environmental micropolarity and for testing their permeability to water.

## ACKNOWLEDGMENT

We are grateful to Drs. J. Gallay, M. Vincent, and J. C. Brochon for their help in recording fluorescence decays with the LURE apparatus, for the analysis of the data with the maximum entropy method, and for fruitful discussions. Our thanks to J. Robb for rereading the English manuscript.

## REFERENCES

Bittman, R., & Blau, L. (1972) *Biochemistry 11*, 4831–4839.
Blatt, E., & Sawyer, W. H. (1985) *Biochim. Biophys. Acta 822*, 43–62.
Blume, A. (1983) *Biochemistry 22*, 5436–5442.
Catteral, R., & Duddel, D. A. (1983) in *Time-Resolved Fluorescence Spectroscopy in Biochemistry and Biology* (Cundall, R. B., & Dale, R. E., Eds.) NATO Advanced Science Institutes Series A69, pp 173–195, Plenum Press, NY.
Conrad, M. P., & Strauss, H. L. (1985) *Biophys. J. 48*, 117–124.
Deamer, D. W., & Bramhall, J. (1986) *Chem. Phys. Lipids 40*, 167–188.
Deamer, D. W., & Nichols, J. W. (1989) *J. Membr. Biol. 107*, 91–103.
de Bony, J., & Tocanne, J. F. (1983) *Chem. Phys. Lipids 32*, 105–121.
de Bony, J., & Tocanne, J. F. (1984) *Eur. J. Biochem. 143*, 373–379.
de Bony, J., Lopez, A., Gilleron, M., Welby, M., Lanéelle, G., Rousseau, B., Beaucourt, J. P., & Tocanne, J. F. (1989) *Biochemistry 28*, 3728–3737.
De Loof, H., Harvey, S. C., Segrest, J. P., & Pastor, R. W. (1991) *Biochemistry 30*, 2099–2113.
Demel, R. A., Kinsky, S. C., Kinsky, C. B., & van Deenen, L. L. M. (1968) *Biochim. Biophys. Acta 150*, 655–665.
Demel, R. A., Bruckdorfer, K. R., & van Deenen, L. L. M. (1972) *Biochim. Biophys. Acta 255*, 321–330.
Diamond, J. M., & Katz, Y. (1974) *J. Membr. Biol. 17*, 121–154.
Dupou, L., Teissié, J., & Tocanne, J. F. (1986) *Eur. J. Biochem. 154*, 171–177.
Dupou-Cézanne, L., Lopez, A., & Tocanne, J. F. (1988) *Eur. J. Biochem. 171*, 669–674.
Egberts, E., & Berendsen, H. J. C. (1988) *J. Chem. Phys. 89*, 3718–3732.
Ferrières, X., Lopez, A., Altibelli, A., Dupou-Cézanne, L., Lagouanelle, J. L., & Tocanne, J. F. (1989) *Biophys. J. 55*, 1081–1091.
Finkelstein, A., & Cass, A. (1968) *J. Gen. Physiol. 52*, 145s–173s.
Fiorini, R. M., Valentino, M., Wang, S., Glaser, M., & Gratton, E. (1987) *Biochemistry 26*, 3864–3870.
Fiorini, R. M., Valentino, M., Glaser, M., Gratton, E., & Curatola, G. (1988) *Biochim. Biophys. Acta 939*, 485–492.
Fiorini, R., Gratton, E., & Curatola, G. (1989) *Biochim. Biophys. Acta 1006*, 198–202.
Flewelling, R. F., & Hubbell, W. L. (1986) *Biophys. J. 49*, 541–552.
Griffith, O. H., Dehlinger, P. J., & Van, S. P. (1974) *J. Membr. Biol. 15*, 159–192.
Katz, Y., & Diamond, J. M. (1974) *J. Membr. Biol. 17*, 101–120.
Knott, R. B., & Schoenborn, B. P. (1986) *Methods Enzymol. 127*, 217–229.
Knutson, J. R., Walbridge, D. G., & Brand, L. (1982) *Biochemistry 21*, 4671–4679.
Kuipers, O. P., Vincent, M., Brochon, J. C., Verheij, H. M., de Haas, G. M., & Gallay, J. (1991) *Biochemistry 30*, 8771–8785.
Lakowicz, J. R. (1983) in *Principles of Fluorescence Spectroscopy*, Vol. 3, pp 51–93, Plenum Press, New York, London.
Lakowicz, J. R., Joshi, N. B., Johnson, M. L., Szmacinski, H., & Gryczynski, I. (1987) *J. Biol. Chem. 262*, 10907–10910.
Lipschitz-Faber, C., & Degani, H. (1980) *Biochim. Biophys. Acta 600*, 291–300.
Livesey, A. K., & Brochon, J. C. (1987) *Biophys. J. 52*, 693–706.
Marqusee, J. A., & Dill, K. A. (1986) *J. Chem. Phys. 85*, 434–444.
Meier, E., Schummer, D., & Sandhoff, K. (1990) *Chem. Phys. Lipids 55*, 103–113.
Milon, A., Lazrak, T., Albrecht, A. M., Wolf, G., Weill, G., Ourisson, G., & Nakatani, Y. (1986) *Biochim. Biophys. Acta 859*, 1–9.
Nagle, J. F. (1987) *J. Bioenerg. Biomembr. 19*, 413–426.
Pérochon, E., & Tocanne, J. F. (1991) *Chem. Phys. Lipids 58*, 7–17.
Pérochon, E., Lopez, A., & Tocanne, J. F. (1991) *Chem. Phys. Lipids 59*, 17–28.
Raudino, A., & Mauzerall, D. (1986) *Biophys. J. 50*, 441–449.
Scherer, J. R. (1989) *Biophys. J. 55*, 957–964.
Schuler, I. S., Milon, A., Nakatani, Y., Ourisson, G., Albrecht, A. M., Benveniste, P., & Hartmann, M. A. (1991) *Proc. Natl. Acad. Sci. U.S.A. 88*, 6926–6930.
Sikaris, K. A., Thulborn, K. R., & Sawyer, W. H. (1981) *Chem. Phys. Lipids 29*, 23–36.
Simon, S. A., & McIntosh, T. J. (1986) *Methods Enzymol. 127*, 511–521.

Straume, M., & Litman, B. J. (1987a) *Biochemistry 26*, 5113–5120.
Straume, M., & Litman, B. J. (1987b) *Biochemistry 26*, 5121–5126.
Szoka, F., Olson, F., Heath, T., Vail, W., Mayhew, E., & Papahadjopoulos, D. (1980) *Biochim. Biophys. Acta 601*, 559–571.
Tanford, C. (1973) in *The Hydrophobic Effect*, John Wiley & Sons, New York.
Thulborn, K. R., Tilley, L. M., Sawyer, W. H., & Treolar, F. E. (1979) *Biochim. Biophys. Acta 558*, 166–178.
Tocanne, J. F., & Teissié, J. (1990) *Biochim. Biophys. Acta 511*, 125–140.
Träuble, H. (1971) *J. Membr. Biol. 4*, 193–208.
Villalain, J., & Prieto, M. (1991) *Chem. Phys. Lipids 59*, 9–16.
Welby, M., & Tocanne, J. F. (1982) *Biochim. Biophys. Acta 689*, 173–176.
Williams, B. W., & Stubbs, C. D. (1988) *Biochemistry 27*, 7994–7999.
Wiener, M. C., King, G. I., & White, S. H. (1991) *Biophys. J. 60*, 568–576.
Worcester, D. L., & Franks, N. P. (1976) *J. Mol. Biol. 100*, 359–378.
Yeagle, P. L. (1985) *Biochim. Biophys. Acta 822*, 267–287.
Zannoni, C. (1983) *Chem. Phys. Lipids 32*, 179–250.
Zolese, G., Gratton, E., & Curatola, G. (1990) *Chem. Phys. Lipids 55*, 29–39.

**Registry No.** Cholesterol, 57-88-5; water, 7732-18-5.